Ferromagnetic moment and antiferromagnetic coupling in (Ga,Mn)As thin films

K. W. Edmonds,[1] N. R. S. Farley,[1] T. K. Johal,[2] G. van der Laan,[2] R. P. Campion,[1] B. L. Gallagher,[1] and C. T. Foxon[1]
[1]*School of Physics and Astronomy, University of Nottingham, Nottingham NG7 2RD, United Kingdom*
[2]*CCLRC Daresbury Laboratory, Warrington WA4 4AD, United Kingdom*
(Received 8 October 2004; published 28 February 2005)

We demonstrate that carefully prepared (Ga,Mn)As films can show large magnetic moments per atom across a wide range of Mn concentrations, indicating almost full participation of the Mn in the ferromagnetism. Applying sum rules to Mn $L_{2,3}$ x-ray magnetic circular dichroism (XMCD) spectra yields a magnetic moment per Mn of around $4.5\mu_B$, including a small positive orbital moment. We also present direct evidence for antiferromagnetic coupling between interstitial and substitutional Mn in unannealed (Ga,Mn)As. The Mn $L_{2,3}$ x-ray absorption line shapes display no sizeable site or concentration dependence, but in unannealed (Ga,Mn)As the XMCD signal is significantly smaller, and increases linearly under high magnetic fields.

DOI: 10.1103/PhysRevB.71.064418 PACS number(s): 75.50.Pp, 71.20.Nr, 78.70.Dm

Combining the electronic and optical properties of semiconductors with magnetic phenomena leads to unusual possibilities for integrated storage and processing technologies. The discovery that the canonical semiconductor GaAs can be made ferromagnetic by doping with a few percent Mn[1] represented an important breakthrough in this field. Mn incorporated substitutionally in GaAs is an acceptor as well as a $J=5/2$ moment, and the ferromagnetism is driven by local interactions between Mn moments and GaAs valence band holes. Clear correlation between the ferromagnetic transition temperature and the hole concentration has been demonstrated in a number of experimental studies.[2–5] However, a deeper understanding of the magnetic order is essential for harnessing the full potential of this material.

The Mn magnetization and its dependence on field and temperature have emerged as key issues in theoretical and experimental studies of (Ga,Mn)As. Competition between antiferromagnetic and hole-mediated ferromagnetic interactions of substitutional Mn may lead to magnetic frustration, and a reduction of the net Mn magnetic moment μ from its atomic value of $5\mu_B$ per atom.[6] Moreover, at high hole densities, the Mn has a tendency to autocompensate by occupying donor interstitial sites, and the formation of antiferromagnetically coupled donor-acceptor pairs is predicted.[7–9] Anisotropy of Mn—Mn interactions may be a further source of spin disorder.[10] Experimentally, an apparent "magnetization deficit" of more than 50% (i.e., $\mu \leqslant 2.5\mu_B/\mathrm{Mn}$) has been observed using superconducting quantum interference device (SQUID) magnetometry.[4,11] Understanding and minimizing this effect is vital, since incomplete participation in the ferromagnetism will limit the Curie temperature T_C. However, a quantitative analysis using such bulk-sensitive magnetometry techniques is obscured by uncertainties in the substitutional Mn concentration,[12] as well as various extrinsic contributions to the signal.

The element-specific x-ray magnetic dichroism techniques are a more direct probe of local magnetic moments. In particular, x-ray magnetic circular dichroism (XMCD) in $L_{2,3}$ absorption is widely used for quantitative determination of spin and orbital magnetic moments on a per atom basis, by normalizing to the isotropic x-ray absorption spectrum (XAS) and by applying sum rules.[13] Early XMCD studies of (Ga,Mn)As reported a remarkably large magnetization deficit of up to 85%.[14,15] It has since been shown that these studies mostly measured a Mn-rich surface oxide layer rather than bulk (Ga,Mn)As,[16] illustrating that it is important to have well-prepared samples if one is to obtain quantitative information using XMCD.

Here we report detailed XMCD measurements on a series of high-quality (Ga,Mn)As thin films. We find a large dichroism signal in carefully prepared and annealed samples, revealing large magnetic moments per Mn atom and showing that most of the Mn are coupled ferromagnetically. Before annealing, the XMCD is smaller and weakly field-dependent, demonstrating that a significant fraction of the Mn moments are antiferromagnetically coupled.

The (Ga,Mn)As films are grown by low-temperature (LT) molecular-beam epitaxy (MBE) using As_2.[17] The layer structure is 50 nm (Ga,Mn)As/50 nm LT-GaAs/100 nm MBE GaAs/semi-insulating GaAs(100) substrate. The quoted Mn concentrations are obtained from the Ga/Mn flux ratio, calibrated by secondary ion mass spectrometry measurements on 1 μm thick samples grown under the same conditions. The quoted values therefore correspond to the *total* Mn concentration in the films, before any annealing or etching procedure. We expect that the concentration of substitutional Mn will be smaller than the quoted values, since some of the incorporated Mn may occupy interstitial sites, clusters, or surface aggregates. After growth, samples are annealed in air at 190 °C for around 100 h. This is an established method for increasing both T_C and the hole density. The mechanism appears to be the removal of compensating donor interstitial Mn, which is weakly bound and can diffuse relatively freely to the surface at these temperatures.[8,18] T_C values are obtained both from anomalous Hall effect and magnetometry measurements, and are consistent with the trends discussed in detail in Ref. 12.

Mn $L_{2,3}$ XAS and XMCD spectra are recorded using $99\% \pm 1\%$ circularly polarized x rays from beamline ID8 at the European Synchrotron Radiation Facility. Magnetic fields of up to 5 T are applied parallel and antiparallel to the photon helicity vector, obtaining spectra for all four alignments of the field and helicity vector. To remove the surface Mn-

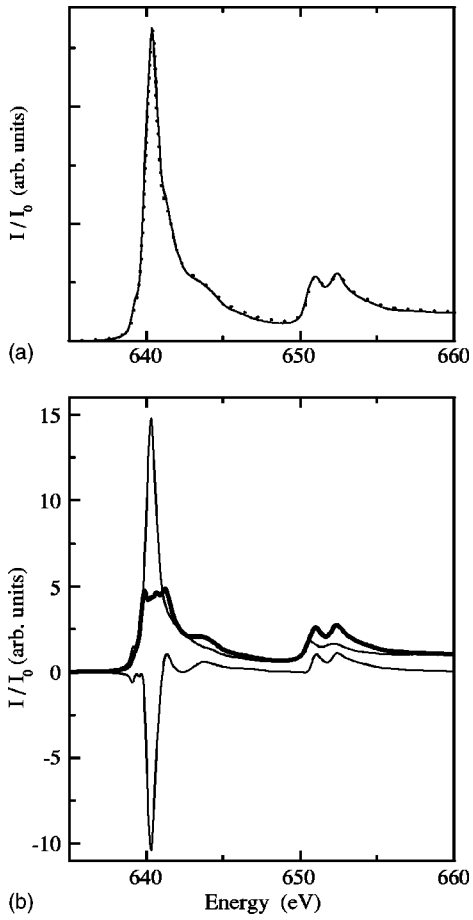

FIG. 1. (a) Mn $L_{2,3}$ XAS for annealed (full lines) and unannealed (dots) unmagnetized (Ga,Mn)As thin films with nominal Mn concentration 8.4%. (b) Mn $L_{2,3}$ XAS from the annealed film, for parallel and antiparallel helicity and magnetization, as well as the difference spectrum (XMCD).

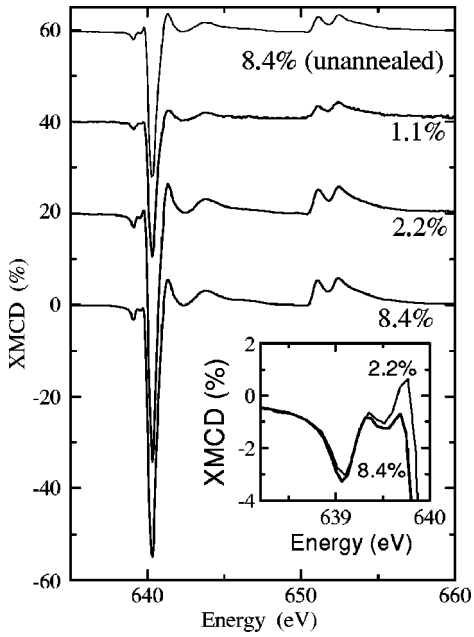

FIG. 2. Mn $L_{2,3}$ XMCD spectra, normalized to the L_3 peak of the summed spectra, for (Ga,Mn)As films with nominal Mn concentrations 8.4%, 2.2%, 1.1%, and 8.4% (unannealed). The spectra are offset for clarity. The L_3 pre-edge region for the annealed 8.4% and 2.2% films are compared in the inset.

rich oxidized layer, the samples are briefly etched in concentrated HCl and rinsed in de-ionized water, just prior to loading into the UHV superconducting magnet vessel where the measurements are performed. Data are obtained both in fluorescence and total electron yield (TEY) modes. Both methods are found to give similar results. This is in spite of the different probing depths of the two techniques and is in contrast to other reports, illustrating the high uniformity of the Mn distribution in the present samples after etching. Only the TEY results are presented here, as these show the higher signal-to-noise ratio.

Figure 1(a) shows the unmagnetized Mn $L_{2,3}$ XAS of annealed (T_C=145 K) and unannealed (T_C=55 K) (Ga,Mn)As films with nominal 8.4% Mn, after HCl etching. A linear background is subtracted, and the data are normalized to a unity edge jump. The spectra are similar to the calculated spectrum for the hybridized state reported in Ref. 16, with rather indistinct multiplet splitting compared to MnO, but with a large branching ratio compared to metallic Mn.[19] This is in contrast to earlier x-ray absorption studies of (Ga,Mn)As, where a pronounced multiplet structure was observed,[14,15] which is probably attributable to surface oxidation. We ascribe the suppression of the multiplet structure in (Ga,Mn)As to hybridization with and screening by the mainly As *p* states in the valence band.

Mn $L_{2,3}$ XAS spectra for the annealed (Ga,Mn)As film under parallel and antiparallel field alignment, I^+ and I^-, as well as the difference ($I^+ - I^-$, XMCD) spectrum, are shown in Fig. 1(b). The spectra were measured at a temperature of 6 K and under magnetic fields of ±2 T, applied along the growth direction. This corresponds to the hard magnetic axis of the compressive-strained (Ga,Mn)As film, although the applied field is large enough to overcome the anisotropy field of around 0.7 T. In contrast to the XAS spectra, the XMCD spectral shape is qualitatively similar to the earlier reports.[14–16] This is mainly because XMCD measures only the part of the sample with a net magnetic polarization, and so in contrast to the XAS spectra is not "polluted" by the contaminated nonmagnetic surface contributions. Most of the features of the XMCD spectrum are similar to those calculated for a pure d^5 ionic state,[20] and observed for, e.g., dilute Mn adsorbates on Fe,[21,22] or Mn impurities in noble metals.[23] The exception is the small pre-edge peak at around 639.1 eV (shown on an expanded scale in the inset of Fig. 2), which is not evident in Refs. 21–23. This feature is present in previously reported XMCD spectra from (Ga,Mn)As,[14–16] and is clearly resolved in the present data. This may result from the larger crystal field interaction in (Ga,Mn)As than in the metallic systems, since a similar pre-edge feature emerges in calculated Mn d^5 spectra on increasing the crystal field parameter.[20]

While the shape of the XMCD spectrum is similar to previous reports for (Ga,Mn)As, its magnitude is much larger, indicating a large magnetic moment per Mn atom and a high degree of participation in the ferromagnetism. The maximum

/of the asymmetry, $(I^+-I^-)/(I^++I^-)$, at the L_3 peak is 0.55 ± 0.01, compared to, e.g., ~0.1 in Ref. 14. The spin and orbital magnetic moments per atom, μ_s and μ_l, in the ferromagnetic phase can in principle be quantified by applying the XMCD sum rules.[13] There are several complications to this procedure. First, obtaining the spin moment requires separate integration over each of the spin-orbit split core levels; however, the $2p$-$3d$ Coulomb interaction leads to mixing of the $j=3/2$ and $j=1/2$ manifolds, so that accurate separation may not be possible. A further complication is the contribution from the magnetic dipole term to the spin sum rule, although this effect should be small for Mn substituted in bulk GaAs. Finally, in the sum rules both μ_s and μ_l are proportional to n_h/A, where n_h is the number of unoccupied Mn $3d$ states and A is the integrated area of the magnetization-averaged signal. Determination of the latter requires subtraction of the background and edge steps, which is a significant source of error at these low Mn concentrations.

Here, we subtract edge steps from the normalized absorption spectrum using a similar procedure to that outlined in Ref. 24. We use a value of $n_h=4.9$, i.e., assuming a $3d$ electron count of 5.1. This value has been inferred from the $L_{2,3}$ edge position and lineshape,[14,16] as well as from photoemission measurements.[25] Applying the orbital moment sum rule gives $\mu_l=+(0.16\pm0.02)\mu_B$/Mn. The small positive value of μ_l justifies our assumption of a d electron count slightly higher than 5, in which case the spin and orbital moments are coupled parallel. For μ_s, we take the cutoff for the L_3 dichroism to be the point just before the onset of the L_2 absorption edge, at 650 eV. Then, the value obtained from the sum rule requires a correction factor due to the large mixing of $j=3/2$ and $j=1/2$ levels for the Mn $L_{2,3}$ edges. By comparing calculated spectra with their corresponding ground-state magnetic moments, we derive a correction factor of 1.47, resulting in a spin magnetic moment $\mu_s=(4.3\pm0.3)\mu_B$/Mn. This is similar to the value obtained by comparing the measured asymmetry to the calculated value for full magnetization using the method in Refs. 14 and 22. The ratio μ_l/μ_s is obtained as 0.037 ± 0.002, which is independent of n_h and A, but is affected by the correction factor applied to the spin moment.

The total moment $\mu_{\text{total}}=\mu_s+\mu_l$ per Mn of around $4.5\mu_B$ is larger than the value typically obtained from bulk magnetometry.[4,11] However, it should be recognized that the bulk magnetometry measurements are normalized to the total Mn concentration, some of which will occupy interstitial sites or will have aggregated on the surface, and will not contribute to the ferromagnetic signal. Here, the interstitial and surface Mn has been removed by annealing and etching, and so do not contribute to the measured absorption signal. Normalizing the bulk magnetometry signal to the concentration of magnetically active substitutional Mn, estimated from Hall effect measurements of the carrier density, leads to estimates of the moment which are in agreement with the value obtained here.[12] Additionally, the polarized valence holes introduced by the Mn acceptors have at least partially As $4p$ character, leading to an As moment of opposite sign to the Mn moment. Mn $L_{2,3}$ XMCD distinguishes the Mn local moment from this contribution, although the As moment can in principle also be obtained by measuring the XMCD at the As absorption edges.[26] Note that the large magnetic anisotropy effects observed in (Ga,Mn)As are usually ascribed to the large spin-orbit interaction of the GaAs valence states;[27] however, the nonzero Mn orbital moment found here demonstrates the existence of spin-orbit effects directly associated with the Mn, which may also influence the magnetic anisotropy.

Large XMCD signals are also observed in other films studied. In Fig. 2, the XMCD spectrum for the 8.4% sample shown in Fig. 1 is compared to spectra for samples with 1.1% and 2.2% Mn. For all these measurements the temperature is 6 K and the magnetic field is ±2 T, applied along the surface normal. The spectra are normalized to the same L_3 peak intensity of the summed spectra. The magnitude of the XMCD spectra is similar for the 2.2% and 8.4% samples, with a maximum XMCD asymmetry of ~55%. Consequently, applying sum rules yields a ferromagnetic moment per Mn atom of $\sim4.5\mu_B$ also for the 2.2% sample. A significant difference between the two spectra is only observed at the L_3 pre-edge feature, expanded in the inset of Fig. 2. The pre-edge feature is negative across the whole energy range for the 8.4% sample, while a positive peak around 639.7 eV is observed for the 2.2% sample. Aside from this small difference, all the main features in the XMCD spectra at 8.4% Mn are also observed at 2.2% Mn.

The maximum asymmetry for the 1.1% sample is only ~0.3. However, the T_C for this sample is only 10 K, so that at the measurement temperature of 6 K, a significant reduction of the magnetization from its zero-temperature value is expected. The reduced XMCD signal for this sample may thus be attributed to incomplete saturation of the magnetization due to thermal disorder. The XMCD line shape of the 1.1% sample shows all the same features as those for higher Mn concentrations. Also, the isotropic XAS shows the same "hybridized" shape, with no distinct multiplet structure. Therefore, these measurements do not reveal any substantial differences in the electronic structure of the Mn on either side of the metal-insulator transition, which occurs for Mn concentrations between 1.1% and 2.2% in the present series of samples.

Also shown in Fig. 2 is the normalized XMCD spectrum for the unannealed 8.4% Mn sample. The XMCD line shape is similar to those of the other samples. However, the peak XMCD asymmetry is only 0.32, i.e., 42% smaller than the value obtained for the annealed samples. Before annealing, a significant fraction of the Mn measured in the raw XAS signal will occupy interstitial sites, which do not couple ferromagnetically. This may at least partially account for the reduced XMCD signal. However, all (Ga,Mn)As films studied are highly p-type, and since the interstitial is a double donor and the substitutional a single acceptor, this puts an upper limit on the interstitial concentration of one third of the total concentration. In fact, the interstitial concentration is usually found to be no more than 10%–20% of the total.[12,18] Therefore, other effects are also contributing to the reduced XMCD signal, possibly including antiferromagnetic coupling between interstitial and substitutional Mn,[7] and magnetic frustration due to high carrier compensation.[6,11] Note that no significant differences are observed between the unmagnetized XAS line shapes obtained from annealed and

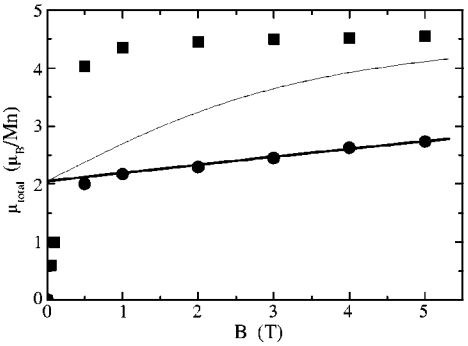

FIG. 3. Field dependence at 6 K of the net magnetic moment per Mn obtained from the XMCD sum rules, in annealed (squares) and unannealed (dots) (Ga,Mn)As samples with nominal 8.4% Mn. The slow approach to saturation in the unannealed case is compared to the $J=5/2$ Brillouin function (thin line) and a modified Brillouin function with an effective temperature of 28 K (thick line).

unannealed samples, as shown in Fig. 1, even though we expect a significantly larger contribution from interstitial Mn in the latter case. However, both interstitial and substitutional Mn in (Ga,Mn)As have nominal valency 2+ (if fully ionized) and tetrahedral coordination,[7] so that the $L_{2,3}$ XAS is not expected to show sizeable site dependence.

We next discuss the magnetic field dependence of the XMCD at 6 K for the annealed and unannealed films. The measured spin-to-orbital moment ratio is unchanged within the experimental error across the whole field range studied. However, the magnitude of the XMCD, and thus the net magnetic moment per Mn obtained from the XMCD sum rules, shows a pronounced field dependence, as shown in Fig. 3. For both films, the XMCD signal increases rapidly initially, as the ferromagnetic magnetization is aligned along the measurement axis, which is the hard magnetic axis in both cases. Then, for the annealed film, the net moment increases by only $\sim 2\%$ on increasing the field from 2 to 5 T, while for the unannealed film the moment increases by 16% over the same field range. The net moment in the unannealed film increases approximately as a_0+a_1B, with $a_0=2.1\mu_B$ and $a_1=0.13\mu_B/\mathrm{T}$. This gradient is significantly smaller than the $J=5/2$ Brillouin function at this temperature (thin line in Fig. 3), indicating that the magnetic signal cannot be described simply as a sum of ferromagnetic plus paramagnetic contributions, and significant antiferromagnetic interactions are present. Instead, we use a modified Brillouin function with an effective temperature $T+T_{\mathrm{AF}}$, where T_{AF} represents the antiferromagnetic coupling strength.[28] This procedure has previously been applied to magnetization curves from insulating (Ga,Mn)As samples, where a T_{AF} of ~ 2.5 K was obtained.[29] In the present case, a T_{AF} of 22 K describes the slow approach to saturation (thick line in Fig. 3). Such a large T_{AF} is unlikely to follow from the rather weak antiferromagnetic interactions between well-separated substitutional Mn, and indeed, samples in which the ferromagnetic coupling due to polarized holes has been suppressed by exposure to hydrogen plasma show a paramagnetic response (i.e., $T_{\mathrm{AF}}\sim 0$ K).[30] This therefore gives important support to theoretical predictions of antiferromagnetic coupling of nearest neighbor interstitial-substitutional pairs.[7–9] We note that such a weak linear increase of magnetization would be extremely difficult to detect with conventional magnetometry techniques, due to the large substrate contribution to the signal.

To summarize, our measurements demonstrate that the ferromagnetic Mn moments in (Ga,Mn)As can be large, even approaching the atomic value. Magnetic frustration and the so-called "magnetization deficit" need not be significant if the (Ga,Mn)As is carefully prepared. In annealed films with both low ($\sim 2.2\%$) and high ($\sim 8.4\%$) Mn concentrations, we observe a net magnetization of around $4.5\mu_B$ per Mn, although obtaining this result using XMCD requires removal of contaminated surface layers. We also observe a small positive orbital contribution to the Mn magnetic moment, not expected if the Mn is in a pure d^5 high-spin state, with an orbital-to-spin moment ratio of ~ 0.037. Before annealing, we observe a clear signature of antiferromagnetic coupling: the Mn moment per atom is significantly reduced compared to the annealed films, and increases slowly and linearly on increasing the magnetic field from 2 to 5 T at temperatures well below T_C. Applying a modified Brillouin function yields an antiferromagnetic coupling temperature of 22 K. We ascribe this antiferromagnetic coupling to the presence of interstitial-substitutional pairs, which break upon annealing.

We wish to thank Julio Cezar, Peter Bencok, Kenneth Larsson, and Nick Brookes for invaluable assistance with the measurements. Funding from EPSRC and the Royal Society (UK) is acknowleged.

[1] H. Ohno, A. Shen, F. Matsukura, A. Oiwa, A. Endo, S. Katsumoto, and Y. Iye, Appl. Phys. Lett. **69**, 363 (1996).

[2] H. Ohno, D. Chiba, F. Matsukura, T. Omiya, E. Abe, T. Dietl, Y. Ohno, and K. Ohtani, Nature (London) **408**, 944 (2000).

[3] F. Matsukura, H. Ohno, A. Shen, and Y. Sugawara, Phys. Rev. B **57**, R2037 (1998).

[4] S. J. Potashnik, K. C. Ku, R. Mahendiran, S. H. Chun, R. F. Wang, N. Samarth, and P. Schiffer, Phys. Rev. B **66**, 012 408 (2002).

[5] K. W. Edmonds, K. Y. Wang, R. P. Campion, A. C. Neumann, C. T. Foxon, and B. L. Gallagher, Appl. Phys. Lett. **81**, 3010 (2002).

[6] J. Schliemann and A. H. MacDonald, Phys. Rev. Lett. **88**, 137 201 (2002).

[7] J. Blinowski and P. Kacman, Phys. Rev. B **67**, 121 204(R) (2003).

[8] K. W. Edmonds, P. Bogusławski, K. Y. Wang, R. P. Campion, S. N. Novikov, N. R. S. Farley, B. L. Gallagher, C. T. Foxon, M. Sawicki, T. Dietl, M. B. Nardelli, and J. Bernholc, Phys. Rev. Lett. **92**, 037 201 (2004).

[9] J. Maŝek and F. Máca, Phys. Rev. B **69**, 165 212 (2004).
[10] G. Zarand and B. Janko, Phys. Rev. Lett. **89**, 047 201 (2002).
[11] P. A. Korzhavyi, I. A. Abrikosov, E. A. Smirnova, L. Bergqvist, P. Mohn, R. Mathieu, P. Svedlindh, J. Sadowski, E. I. Isaev, Y. K. Vekilov, and O. Eriksson, Phys. Rev. Lett. **88**, 187 202 (2002).
[12] K. Y. Wang, K. W. Edmonds, R. P. Campion, B. L. Gallagher, N. R. S. Farley, C. T. Foxon, M. Sawicki, P. Boguslawski, and T. Dietl, J. Appl. Phys. **95**, 6512 (2004).
[13] B. T. Thole, P. Carra, F. Sette, and G. van der Laan, Phys. Rev. Lett. **68**, 1943 (1992); P. Carra, B. T. Thole, M. Altarelli, and X. Wang, *ibid.* **70**, 694 (1993).
[14] H. Ohldag, V. Solinus, F. U. Hillebrecht, J. B. Goedkoop, M. Finazzi, F. Matsukura, and H. Ohno, Appl. Phys. Lett. **76**, 2928 (2000).
[15] S. Ueda, S. Imada, T. Muro, Y. Saitoh, S. Suga, F. Matsukura, and H. Ohno, Physica E (Amsterdam) **10**, 210 (2001).
[16] K. W. Edmonds, N. R. S. Farley, R. P. Campion, C. T. Foxon, B. L. Gallagher, T. K. Johal, G. van der Laan, M. MacKenzie, and J. N. Chapman, Appl. Phys. Lett. **84**, 4065 (2004).
[17] R. P. Campion, K. W. Edmonds, L. X. Zhao, K. Y. Wang, C. T. Foxon, B. L. Gallagher, and C. R. Staddon, J. Cryst. Growth **247**, 42 (2003).
[18] K. M. Yu, W. Walukiewicz, T. Wojtowicz, I. Kuryliszyn, X. Liu, Y. Sasaki, and J. K. Furdyna, Phys. Rev. B **65**, 201 303(R) (2002).
[19] Y. Yonamoto, T. Yokoyama, K. Amemiya, D. Matsumura, and T. Ohta, Phys. Rev. B **63**, 214 406 (2001).
[20] G. van der Laan and B. T. Thole, Phys. Rev. B **43**, 13 401 (1991); these calculations consider a crystal field of octahedral symmetry, however, the pre-edge feature also emerges in tetrahedral symmetry, as seen from the XAS calculations in G. van der Laan and I. W. Kirkman, J. Phys.: Condens. Matter **4**, 4189 (1992).
[21] H. A. Dürr, G. van der Laan, D. Spanke, F. U. Hillebrecht, and N. B. Brookes, Phys. Rev. B **56**, 8156 (1997).
[22] J. Dresselhaus, D. Spanke, F. U. Hillebrecht, E. Kisker, G. van der Laan, J. B. Goedkoop, and N. B. Brookes, Phys. Rev. B **56**, 5461 (1997).
[23] W. D. Brewer, A. Scherz, C. Sorg, H. Wende, K. Baberschke, P. Bencok, and S. Frota-Pessoa, Phys. Rev. Lett. **93**, 077 205 (2004).
[24] C. T. Chen, Y. U. Idzerda, H.-J. Lin, N. V. Smith, G. Meigs, E. Chaban, G. H. Ho, E. Pellegrin, and F. Sette, Phys. Rev. Lett. **75**, 152 (1995).
[25] J. Okabayashi, A. Kimura, T. Mizokawa, A. Fujimori, T. Hayashi, and M. Tanaka, Phys. Rev. B **59**, R2486 (1999).
[26] D. J. Keavney, D. Wu, J. W. Freeland, E. Johnston-Halperin, D. D. Awschalom, and J. Shi, Phys. Rev. Lett. **91**, 187 203 (2003).
[27] T. Dietl, H. Ohno, and F. Matsukura, Phys. Rev. B **63**, 195 205 (2001).
[28] J. Gaj, R. Planel, and G. Fishman, Solid State Commun. **29**, 435 (1979).
[29] A. Oiwa, S. Katsumoto, A. Endo, M. Hirosawa, Y. Iye, H. Ohno, F. Matsukura, A. Shen, and Y. Sugawara, Solid State Commun. **103**, 209 (1997).
[30] S. T. B. Goennenwein, T. A. Wassner, H. Huebl, M. S. Brandt, J. B. Philipp, M. Opel, R. Gross, A. Koeder, W. Schoch, and A. Waag, Phys. Rev. Lett. **92**, 227 202 (2004).